

A modified quasi-static model with lateral stiffness deterioration mechanism for self-centering concrete pier

H. Liu¹, M. He^{1,3,*}, J. Guo^{1,2}, Y. Shi¹, Zh. Hou³

Received: July 2012, Revised: November 2013, Accepted: June 2014

Abstract

Self-centering pier (SCP) has been viewed as a remarkable accomplishment which is able to sustain major lateral loading with reduced structure damage in seismic engineering. Stiffness deterioration observed in experiment is vital for the seismic performance of self-centering concrete pier. In this contribution, the associated stiffness deterioration with respect to the structural damage is modeled in a modified analytical model for SCP comprehensively. In the proposed modified theoretical model, the lateral force-displacement relation associated with the stiffness reducing is analyzed. Three damage factors are introduced in the stiffness deterioration analysis to illustrate the damage evolution caused by gradually increasing lateral displacement. The proposed modified quasi-static model with damage evolution or stiffness deterioration has been validated against an experiment we conducted, where a good agreement is clearly evident. Subsequently, a parametric investigation focusing on aspect ratio, initial pre-tension, and ratio of ED (Energy Dissipator) was conducted to evaluate the hysteretic behavior of SCP under quasi-statically cyclic loading.

Keywords: Self-centering pier, Stiffness deterioration, Residual displacement, Damage; quasi-static.

1. Introduction

Performance-based design is being paid more and more attention by the colleagues in earthquake engineering, attempting to predict and control better the post-earthquake functionality of structures. In the recent serious earthquakes occurred around the world, such as American Northridge 1994, Japanese Kobe 1995, Chinese Wenchuan 2008 earthquake (see Wang (2008)^[1], Yen et al (2009)^[2] etc., the bridge structures located in the earthquake-affected area have seriously suffered tremendous damage, further directly or indirectly caused huge losses to economy and society. The critical destruction left bridges unusable until repairs can be made several months later, leading to the great difficulties for the earthquake relief such as rescue and supplies transportation. The long-lasting pain from the disasters forced people to realize that the collapse prevention philosophy of designing is not sufficient in the modern society with diverse need for safety. The collapse prevention philosophy should be implemented as the bottom line in design.

Performance based design based on the user customized

philosophy is an alternative practical approach to implement a customized level of post earthquake performance into design.

Bridges as critical links in the transportation network must remain intact or repairable so that emergency services can be provided immediately following an earthquake. Bridges are expected to maintain suitable post-earthquake performance to sustain aftershocks. Kawashima et al (1998)^[3] reported that following the Kobe earthquake, over 100 reinforced concrete (RC) columns with a residual drift of over 1:5% column height were demolished even though they did not collapse. After that, residual displacements is gradually accepted as a meaningful indicator of the post-earthquake ability of piers damaged in an earthquake to resist aftershocks (see Bazzurro, Cornell et al. (2004)^[9]; Luco, Bazzurro et al. (2004)^[4]; Lee and Billington (2011)^[5]; Guo (2012)^[6]; He et al. (2012)^[7]).

1.1. Evolution from collapse prevention philosophy to customized performance-based philosophy

In US, China and many other countries around the world, the concrete piers have been widely used in the traffic lifeline bridges, due to its sufficient load-bearing capacity and economical efficiency.

Based on collapse prevention philosophy, concrete piers are typically designed such that plastic behavior will concentrate in the columns (plastic hinge region) during earthquakes on seismic precautionary level. The piers are designed to undergo inelastic deformations under severe

* Corresponding author: heminghua@tsinghua.edu.cn

1 Department of Civil Engineering, Tsinghua University, Beijing 100084, China

2 Research Institute of Highway Ministry of Transport, Beijing 100088, China

3 Central Research Institute of Building and Construction Co., Ltd., MCC, Beijing 100023, China

earthquakes. Actually, ductility design based on collapse prevention philosophy may withstand a rare earthquake. However irreparable structural damage should occur inevitably as a result of the appreciable inelastic behavior. Permanent or residual displacement can be left as an important indicator of post-earthquake functionality in bridges. Besides, the residual displacement could assist in determining whether or not a bridge remains usable following an earthquake.

The ideal expectation of seismic design requires not only less the structural damage, but also a minor cost of repairing and socio-economic impact even under severe earthquake. To this end, on the basis of the avoidance of collapse, minimization of the interruption of the infrastructures like bridges should be taken into major consideration. The performance-based philosophy allows the owner of the structure to customize the performance even before the design stage. For lifeline projects such as highway network etc., it is desirable to have bridges that can remain operational and limit the downtime after a seismic event, requiring the bridge effectively combine the elastic self-centering capacity to reduce the residual displacement and sufficient inelastic energy dissipation capacity to resist the earthquake.

1.2. Recent developments of self-centering piers and related structures

First in the Japanese Code (see Kawashima (1997)^[8]), a definition of the residual displacement has been introduced as one of fundamental measures of post-earthquake bridge functionality, which indicates whether or not a bridge remains usable after an earthquake. During last decade, series of investigations (including MacRae and Kawashima (1997)^[15]; Pampanin, Christopoulos et al. (2002)^[21]; Christopoulos and Pampanin (2004)^[12]; Palermo, Pampanin and Calvi (2005)^[18]; Lee and Billington (2011)^[5]) have been focusing on controlling residual displacement, which should be considered as a valid complementary indicator of seismic damage with the development of seismic damage indexes.

With the intent to further reduce the level of damage associated to residual (permanent) deformations; more emphasis has thus been recently given to the development of self-centering devices or systems.

In order to reduce the post-earthquake residual displacement with respect to the damage on the pier, the development of self-centering piers has been boosted rapidly in recent years. Some research has been giving emphasis on advanced materials like shape memory alloy that combines self-centering and energy dissipation capabilities, while others on the high-seismic-performance jointed ductile system by using traditional materials and retrofitted pattern to provide energy dissipating and self-centering capacities at the same time. In this new system, the inelastic demand is accommodated within the connection through the opening and closing of an existing gap at the critical interface, which is quite different with the development of a plastic hinge in a rigid joint system (see Palermo

and Pampanin (2008)^[17]). With an appropriate ratio between restoring moment provided by post-tensioning and dissipative moment provided by energy dissipation devices, a satisfactory combination of self-centering and energy dissipation capacities can be guaranteed (see Palermo, Pampanin and Carr (2005)^[20]). Based on this, a typical flag-shape hysteretic response can be obtained as shown in Fig. 2, which indicates negligible residual displacement after external excitation. In addition, the experimental test, comparing single self-centering bridge piers with monolithic counterparts, has been conducted by Palermo, Pampanin and Marriott (2006)^[19], which successfully demonstrated the viability and efficiency of the self centering seismic system. And in the latest research, the assessment of seismic damage significantly exposed the weakness of traditional monolithic piers. In the seismic cases where residual displacement ratio exceeds 1%, which is almost inevitable for rigid joint piers after a severe earthquake, the functionality of these bridges would be questionable and huge socio-economic loss would come subsequently (see Lee and Billington (2011)^[5]).

1.3. Scope of the study and paper organization

On the basis of aforementioned previous research, plenty of experimental and numerical studies on the seismic performance of self-centering concrete pier systems have been carried out. While a set of constructive accomplishments have been achieved (see Billington and Yoon (2004)^[10]; Kim and Christopoulos (2008)^[14]; Marriott, Pampanin and Palermo (2009)^[16]). In the aspect of quasi-static response model, a typical half-cycle hysteretic response of steel truss pier has been illustrated (Pollino and Bruneau (2007)^[22]). And a quasi-static response model of segmental precast unbonded posttensioned concrete bridge columns for static pushover analysis was well developed in previous study (Ou, Chiewanichakorn, Aref and Lee (2007)^[23]; Yu-Chen Ou, Mu-Sen Tsai, Kuo-Chun Chang, George C. Lee (2010)^[27]). However, the attention on the quasi-static response model, especially for cyclic loading analysis including the stiffness deterioration evolution, for self-centering concrete piers is considerably insufficient.

In this study, the behavior of a concrete pier with extra pretension provided by unbonded posttensioned tendon was comprehensively evaluated. The paper is organized as follows: in section 2, a modified quasi-static response model for self-centering concrete piers is developed; based on the associated assumptions, the stiffness deterioration or degrading mechanism for lateral force-displacement is implemented in the proposed model; in section 3, subsequently, a parametric investigation based on the verification of the modified quasi-static response model calibrated by a SCP experiment; and in section 4, the paper is concluded with several remarks.

2. A Modified Quasi-Static Response Model for SCP

2.1. SCP structural components

The typical SCP consists of three main components, the self-centering (SC) component, the energy dissipation (ED) component, and load-bearing (LB) component, as shown in Fig. 1 (See He, Xin and Guo et al. (2010)^[24] and (2012)^[7]). The SC component commonly in the form of post-tensioned tendon which provides self-centering

functionality is designed to behave almost elastically during the whole hysteretic response of self-centering bridge piers, while ED components usually in the form of mild steels serving as passive energy dissipation devices are considered to behave elasto-plastically. The concrete piers not only bear the vertical load from deck, but also carry out a controlled rocking motion between the LB component (i.e. column) and base of piers during an earthquake. With a reasonable ratio between SC and ED components, a typical “fan-bladed” or “flag-shape” hysteretic behavior can be achieved as shown in Fig. 2.

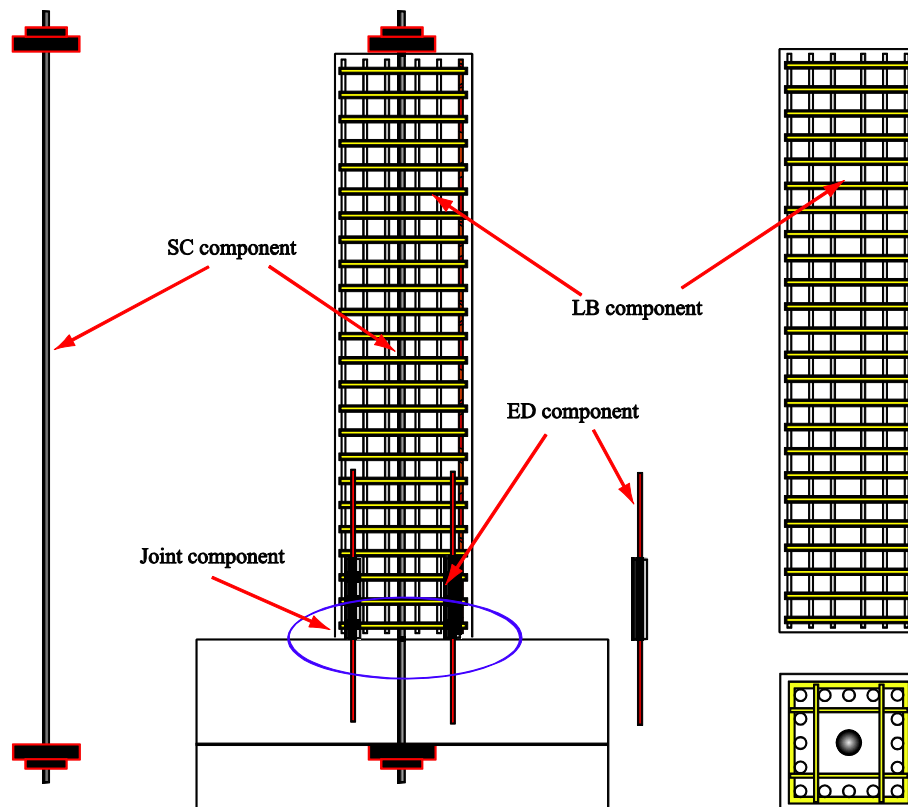


Fig. 1 Fundamental structural components of SCP: SC component, ED component and LB component. (see He et al. (2012)^[7])

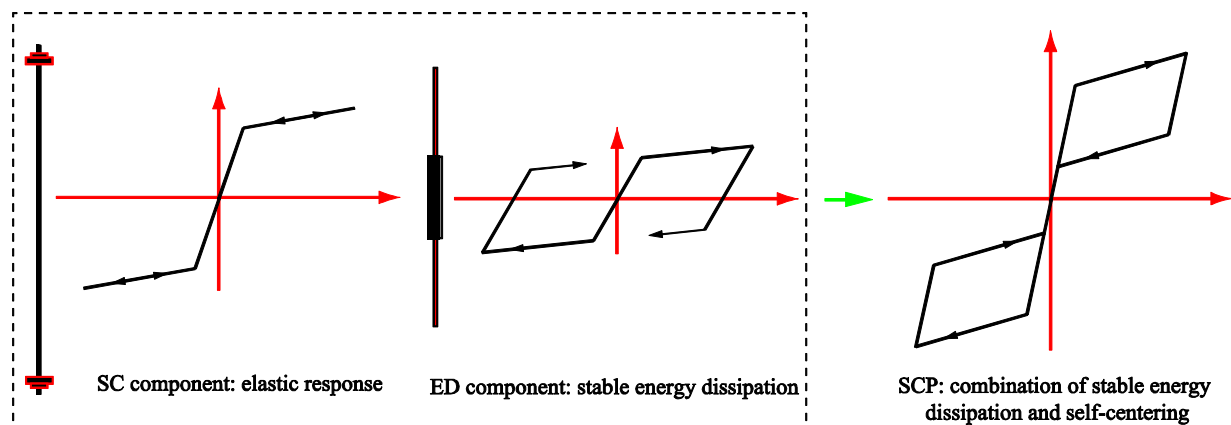


Fig. 2 The basis of the “fan-bladed” or “flag-shape” hysteretic behavior: combined action between SC and ED components. (see He et al. (2012)^[7])

2.2. Assumptions

The rocking center of pier is assumed to be located at the edge of concrete column, and the energy dissipation of

concrete part is neglected because of the opening and closing of an existing gap at the critical joint. The mild steel is partly embedded into concrete pier with an initial unbonded length (l_{u0}) so that they provide appreciable

energy dissipation capacity and ductile deformation capacity.

The model considers motion of the pier only in transverse direction and assumes no interaction with other piers and abutments through the bridge deck. The key parameters for the cyclic hysteretic response of self-centering bridge piers considered here include aspect ratio (h/b), the initial pretension (T_{in}), and the ratio of ED

bar (ρ_{ED}). The various steps during rocking are shown in Fig. 3, and the process repeats itself in symmetry under cyclic loading. There's a transition from first to second-cycle response due to the compression yield of mild steel when the system comes to rest, which results in a conspicuous reduction of uplifting force after second cycle loading.

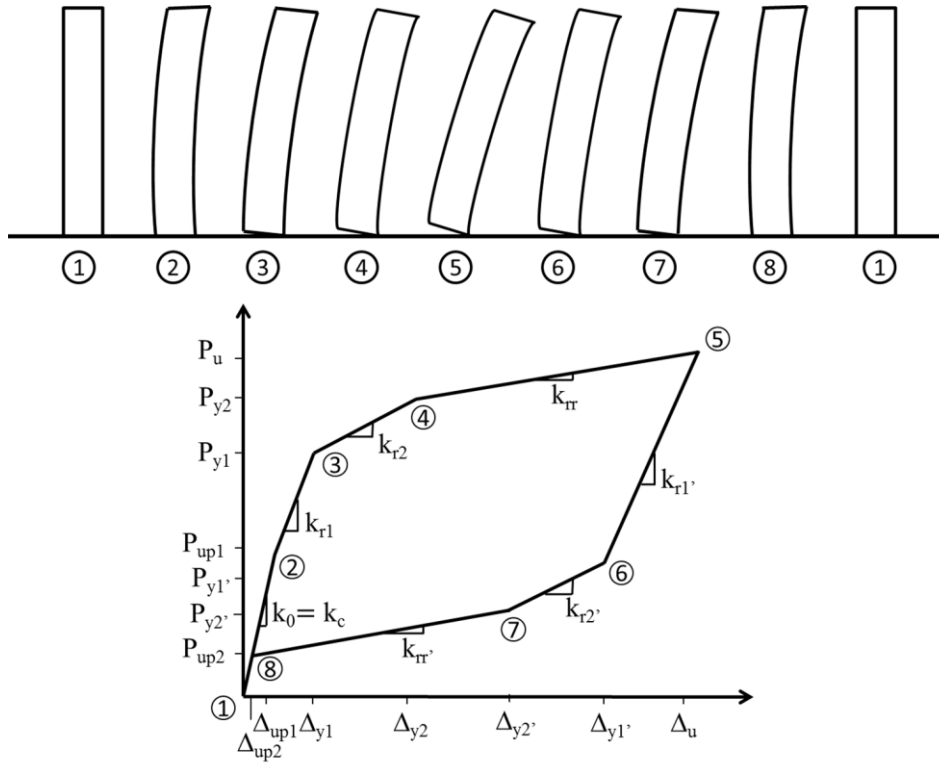


Fig. 3 The modified theoretical model for lateral force-displacement model of SCP

2.3. Stiffness degrading Analysis

During the cyclic loading, a series of inevitable damages will take place according to the severity of lateral excitation. In this study, an equivalent lateral stiffness (ELS) \tilde{k}_c is adopted to show the stiffness degrading process. Assume the pier height h , and the stiffness of post-tensioned tendons k_{SC} remain unchanged, while the initial lateral stiffness k_c , the equivalent lever of force of SC and ED components \tilde{b} , b_{ED1} , and b_{ED2} , and the stiffness of ED bars k_{ED1} k_{ED2} are the functions of the lateral displacement Δ . In the different steps of hysteric cycle, the Equations for calculating ELS are shown in Table. I.

Take three major reasons for stiffness degrading into consideration, and introduce three corresponding damage factors into this study. β_u is defined to describe the elongation of equivalent unbonded length of ED bars (l_{ED}^*) which is caused by cyclic lateral displacement, β_c is defined to reflect the reduction of initial lateral stiffness of

piers (k_c) and β_r is defined to mirror the decrease of equivalent arm of force (\tilde{b} , \tilde{b}_{ED1} , \tilde{b}_{ED2}) caused by the damage of concrete edge, respectively.

- The development of equivalent unbonded length of ED bars l_{ED}^*

Firstly, the damage factor β_u describes the elongation of unbonded length of ED bars. l_{ED}^* will develop with the increase of lateral displacement. During the cyclic loading, the l_{ED}^* of loading and unloading processes are defined as l_{ED+}^* and l_{ED-}^* , respectively.

$$l_{ED+}^* = l_{u0} + 2l_{eu} + \beta_u \frac{\tilde{b}_{ED1}}{h} \Delta_{j-1} \quad (1)$$

$$l_{ED-}^* = l_{u0} + 2l_{eu} + \beta_u \frac{\tilde{b}_{ED1}}{h} \Delta_j > l_{ED+}^* \quad (2)$$

Where l_{ED+}^* is the equivalent unbonded length of ED

bars in j-th cycle's loading process, while l_{EDj}^* is the equivalent unbonded length of ED bars in j-th cycle's unloading process, and l_{u0} is the initial unbonded length of ED bars. An extra unbonded length l_{eu} along which the strain in the bar is uniformly distributed is assumed on each of the two sides of the ED bars and it depends on the diameter and rib pattern of the bars and confinement effect to the bars. The value of l_{eu} is assumed to be one bar

diameter (Raynor et al. (2002)^[26]). Δ_{j-1} and Δ_j are the maximum lateral displacement of piers in (j-1)-th and j-th cycle, respectively. Because $\Delta_j > \Delta_{j-1}$, the value of l_{EDj}^* is bigger than the value of l_{EDj+}^* , which makes a difference in ELS between loading and unloading process in the same cycle.

Table I Equivalent Lateral Stiffness \tilde{k}_c during the loading and unloading case

Steps	equivalent lateral stiffness \tilde{k}_c	Physical description
① → ②	$\tilde{k}_c = k_c$	Loading: before bottom rocking
② → ③	$\tilde{k}_c = k_{r1} = \frac{1}{\frac{1}{k_c} + \frac{h^2}{k_{SC}\tilde{b}^2 + k_{ED1}\tilde{b}_{ED1}^2 + k_{ED2}\tilde{b}_{ED2}^2}}$	Loading: ED bars remain elastic
③ → ④	$\tilde{k}_c = k_{r2} = \frac{1}{\frac{1}{k_c} + \frac{h^2}{k_{SC}\tilde{b}^2 + \alpha_{ED}k_{ED1}\tilde{b}_{ED1}^2 + k_{ED2}\tilde{b}_{ED2}^2}}$	Loading: Half ED bars are plastic
④ → ⑤	$\tilde{k}_c = k_{rr} = \frac{1}{\frac{1}{k_c} + \frac{h^2}{k_{SC}\tilde{b}^2 + \alpha_{ED}k_{ED1}\tilde{b}_{ED1}^2 + \alpha_{ED}k_{ED2}\tilde{b}_{ED2}^2}}$	Loading: All ED bars are plastic.
⑤ → ⑥	$\tilde{k}_c = k_{r1} = \frac{1}{\frac{1}{k_c} + \frac{h^2}{k_{SC}\tilde{b}^2 + k_{ED1}\tilde{b}_{ED1}^2 + k_{ED2}\tilde{b}_{ED2}^2}}$	Unloading: ED bars unload elastically.
⑥ → ⑦	$\tilde{k}_c = k_{r2} = \frac{1}{\frac{1}{k_c} + \frac{h^2}{k_{SC}\tilde{b}^2 + \alpha_{ED}k_{ED1}\tilde{b}_{ED1}^2 + k_{ED2}\tilde{b}_{ED2}^2}}$	Unloading: Half ED bars are plastic.
⑦ → ⑧	$\tilde{k}_c = k_{rr} = \frac{1}{\frac{1}{k_c} + \frac{h^2}{k_{SC}\tilde{b}^2 + \alpha_{ED}k_{ED1}\tilde{b}_{ED1}^2 + \alpha_{ED}k_{ED2}\tilde{b}_{ED2}^2}}$	Unloading: All ED bars are plastic.
⑧ → ①	$\tilde{k}_c = k_c$	Unloading: after bottom rocking

Subsequently, the stiffness of ED components can be calculated by the Equation below.

$$k_{ED1} = k_{ED2} = E_{ED}A_{ED} / l_{EDj}^* \quad (3)$$

where A_{ED} is the cross-sectional area of energy dissipation bars, l_{EDj}^* is the equivalent unbonded length of ED bars in j-th cycle with different value according to loading or unloading process. l_{EDj}^* will get longer after each cycle and subsequently lead to the reduction of the stiffness of ED components, which gives rise to the degrading of ELS in various steps after uplifting. This is

how the elongation of l_{EDj}^* caused by cyclic excitation affects the degrading process of stiffness, and the ELS of unloading process is smaller than that of loading process in the same cycle.

- The development of Lateral Stiffness k_c

Secondly, the damage factor β_C depicts the reduction of initial lateral stiffness of piers. k_c will decrease according to the increase of lateral displacement due to the damage of concrete piers edge. During the cyclic loading, the k_c of loading and unloading processes are defined as

k_c^+ and k_c^- , respectively.

During the cyclic loading, the k_c of loading and unloading process are defined as k_c^+ and k_c^- , respectively.

$$k_{cj}^+ = [1 - \beta_c (\frac{\Delta_{j-1}}{\Delta_u^{\max}})^2] k_{c0} \quad (4)$$

$$k_{cj}^- = [1 - \beta_c (\frac{\Delta_j}{\Delta_u^{\max}})^2] k_{c0} < k_{cj}^+$$

Where k_{cj} is the initial lateral stiffness of piers in j-th cycle's loading process, while k_{cj}^- is the initial lateral stiffness of piers in j-th cycle's unloading process, and k_{c0} is the intact initial lateral stiffness of piers. Δ_u^{\max} is the maximum lateral displacement allowed in China, which is equal to 3.5% of column height (Chinese Code 50011-2010^[11]).

With the development of displacement, k_c becomes smaller after each heavier lateral excitation, and it leads to the degrading of ELS in all steps. The damage factor β_c is critical in this analysis, and it decides how conspicuously the initial stiffness of concrete piers can influence the degrading process of ELS.

- The development of equivalent levers of force \tilde{b} , \tilde{b}_{ED1} , \tilde{b}_{ED2}

Thirdly, the damage factor β_r reflects the decrease of equivalent arm of force caused by the damage accumulation of concrete edge. \tilde{b} , \tilde{b}_{ED1} and \tilde{b}_{ED2} are the equivalent levers of force of post-tensioned tendon, outer ED bars, and inner ED bars, respectively. The value of their loading and unloading process are the functions of Δ_{j-1} and Δ_j shown below.

$$\tilde{b}_+ = \tilde{b}_0 - \beta_r \frac{\Delta_{j-1}}{\Delta_u^{\max}}$$

$$\tilde{b}_- = \tilde{b}_0 - \beta_r \frac{\Delta_j}{\Delta_u^{\max}} < \tilde{b}_+$$

$$\tilde{b}_{ED1+} = \tilde{b}_{ED10} - \beta_r \frac{\Delta_{j-1}}{\Delta_u^{\max}}$$

$$\tilde{b}_{ED1-} = \tilde{b}_{ED10} - \beta_r \frac{\Delta_j}{\Delta_u^{\max}} < \tilde{b}_{ED1+} \quad (5)$$

$$\tilde{b}_{ED2+} = \tilde{b}_{ED20} - \beta_r \frac{\Delta_{j-1}}{\Delta_u^{\max}}$$

$$\tilde{b}_{ED2-} = \tilde{b}_{ED20} - \beta_r \frac{\Delta_j}{\Delta_u^{\max}} < \tilde{b}_{ED2+}$$

Where \tilde{b}_+ , \tilde{b}_{ED1+} and \tilde{b}_{ED2+} are the equivalent levers of force in j-th cycle's loading process, while \tilde{b}_- , \tilde{b}_{ED1-} and \tilde{b}_{ED2-} are the equivalent levers of force in j-th cycle's unloading process, and \tilde{b}_0 , \tilde{b}_{ED10} and \tilde{b}_{ED20} are the intact initial equivalent levers of force.

Consequently, \tilde{b} , \tilde{b}_{ED1} and \tilde{b}_{ED2} will become smaller after each cycle because of the invasion of rotation center, and subsequently lead to the degrading of ELS in various steps after uplifting.

2.4. Lateral force-displacement analysis

- Loading

The initial lateral stiffness of concrete piers (k_c) gives bridges the assurance of serviceability (①), with which the pier performs elastically before uplifting, and it will degrade according to the development of cyclic loading. Uplifting of the pier (②) begins when the restoring moment created by the posttensioned tendon and bridge weight is overcome by the applied horizontal load.

$$P_{up1} = (T_{in} + W) \frac{\tilde{b}}{h} \quad (6)$$

And the displacement at the point of first uplifting is defined by:

$$\Delta_{up1} = \frac{P_{up1}}{k_c} \quad (7)$$

After the uplifting of one edge of concrete column, the mild steel is activated to control the displacement of the rocking pier. And the lateral stiffness of the pier is reduced to k_{r1} , which will remain unchanged until the mild steel located on uplifting side reach its yielding strength (③). The horizontal load at the point of yielding is defined as

$$P_{y1} = \frac{1}{h} [b(T_{in} + W + \varepsilon_{SCy1} E_{SC} A_{SC}) + \tilde{b}_{ED2} A_{ED} f(\varepsilon_{EDy1}) + \tilde{b}_{ED1} A_{ED} f_{EDy}] \quad (8)$$

$$\varepsilon_{ED2y} = \frac{\tilde{b}_{ED2}}{\tilde{b}_{ED1}} \varepsilon_{EDy} \quad (9)$$

$$\varepsilon_{SCy1} = \frac{\tilde{b}}{\tilde{b}_{ED1}} \frac{l_{ED}^*}{l_{SC}} \varepsilon_{EDy} \quad (10)$$

Where l_{SC} and l_{ED}^* are the lengths of unbouded pretension tendon and equivalent unbouded part of mild steel, respectively. ε_{ED2y} is the yielding strain of mild

steel, ε_{SCy1} is the corresponding strain of mild steel located on the inner side, and ε_{SCy1} is the strain increment of post-tensioned tendon at this time. A_{ED} is the sectional area of mild steel on each side, and $f(\varepsilon)$ representing stress in mild steel is a function of strain, f_{EDy} is the yielding stress of mild steel.

The corresponding system yield displacement, and thus the allowed displacement of serviceability states, Δ_{y1} is defined by

$$\Delta_{y1} = \frac{P_{up1}}{k_c} + \frac{P_{y1} - P_{up1}}{k_{r1}} \quad (11)$$

That is, if the horizontal force applied at the top of column is smaller than P_{y1} of first cycle, all elements of the pier behave elastically and the maximum lateral displacement of pier can be limited within Δ_{y1} .

Taking strain hardening in the mild steel into consideration, postelastic stiffness is assumed to be k_{r2} before the yielding of the mild steel located on the inner side (4), which is much smaller than k_{r1} and mainly depends on the post-yield stiffness ratio of mild steel. The remarkable reduction of lateral stiffness would effectively increase the natural period of bridge piers and help it survive in a severe earthquake. When the inner ED bars yield, the second yielding strength is defined as:

$$P_{y2} = \frac{1}{h} [b(T_{in} + W + \varepsilon_{SCy2} E_{SC} A_{SC}) \quad (12)$$

$$+ \tilde{b}_{ED2} A_{ED} f(\varepsilon_{EDy}) + \tilde{b}_{ED1} A_{ED} f(\varepsilon_{EDy2})]$$

$$\varepsilon_{EDy2} = \frac{\tilde{b}_{ED1}}{\tilde{b}_{ED2}} \varepsilon_{EDy} \quad (13)$$

$$\varepsilon_{SCy2} = \frac{\tilde{b}}{\tilde{b}_{ED2}} \frac{l_{ED}^*}{l_{SC}} \varepsilon_{EDy} \quad (14)$$

Ignoring any second-order effects, the pier is assumed to reach its maximum lateral displacement in j -th cycle when $\Delta_u = \Delta_j$. The lateral force comes to its ultimate value in j -th cycle (5), and P_u is defined as:

$$P_u = \frac{1}{h} [b(T_{in} + W + \varepsilon_{SCu} E_{SC} A_{SC}) \quad (15)$$

$$+ \tilde{b}_{ED2} A_{ED} f(\varepsilon_{ED2u}) + \tilde{b}_{ED1} A_{ED} f(\varepsilon_{ED1u})]$$

$$\varepsilon_{SCy1} = \frac{\tilde{b}}{\tilde{b}_{ED1}} \frac{l_{ED}^*}{l_{SC}} \varepsilon_{ED1u} \quad (16)$$

$$\Delta_u = \frac{P_{up1}}{k_c} + \frac{P_{y1} - P_{up1}}{k_{r1}} + \frac{P_{y2} - P_{y1}}{k_{r2}} + \frac{P_u - P_{y2}}{k_{rr}} \quad (17)$$

Where ε_{ED1u} is the corresponding strain in outer mild steel, ε_{ED2u} is the corresponding strain in inner mild steel, and ε_{SCu} is the corresponding strain increment of post-tensioned tendon. With the symmetric cycle loading process and accumulation of equivalent plastic strain, ε_{ED2u} will approach to ε_{ED1u} rapidly.

• Unloading and Second Cycle Loading

As the horizontal force is reduced, the pier first responds elastically with k_{r1} , and the stress of mild steel rapidly take the transition from tension to compression. Until the compression stress of outer side mild steel reaches the equivalent value of its previous tension stress (6), the equivalent plastic strain of mild steel continues to increase. Then the lateral stiffness reduces to k_{r2} , with combination of the elastic response of inner mild steel and the plastic response of outer ones. When the compression stress of inner mild steel reaches the equivalent value of its previous tension stress (7), all ED bars come to plastic response and the lateral stiffness drastically falls to k_{rr} . With the damage development of concrete edge and the accumulation of equivalent plastic strain in loading process, ELS can be easily calculated, which indicates that k_{r1} , k_{r2} , and k_{rr} can be further smaller than k_{r1} , k_{r2} and k_{rr} , respectively.

$$P_{y1'} = \frac{1}{h} [b(T_{in} + W + \varepsilon_{SCy1'} E_{SC} A_{SC}) \quad (18)$$

$$+ \tilde{b}_{ED2} A_{ED} f^*(\varepsilon_{ED1u}) + \tilde{b}_{ED1} A_{ED} f(\varepsilon_{ED1u})]$$

$$P_{y2'} = \frac{1}{h} [b(T_{in} + W + \varepsilon_{SCy2'} E_{SC} A_{SC}) \quad (19)$$

$$+ \tilde{b}_{ED2} A_{ED} f^*(\varepsilon_{ED2u}) + \tilde{b}_{ED1} A_{ED} f(\varepsilon_{ED1u})]$$

where,

$$\varepsilon_{SCy1'} = \varepsilon_{SCu} - \varepsilon_{SCy1}$$

$$f^*(\varepsilon_{ED1u}) = f(\varepsilon_{ED1u}) - 2\varepsilon_{EDy2} E_{ED} \quad (20)$$

$$\varepsilon_{SCy2'} = \varepsilon_{SCu} - \varepsilon_{SCy2}$$

$$f^*(\varepsilon_{ED2u}) = f(\varepsilon_{ED2u}) - 2\varepsilon_{EDy2} E_{ED}$$

Finally, the uplifted edge of concrete pier settles back again with the contact to its base, which makes ELS back to initial one (k_c), and the mild steel in compression inevitably offsets part of bridge weight and pretension. As a result, the pier will be uplifted again with a much smaller horizontal load (P_{up2}) and uplifting displacement (Δ_{up2})

than P_{up1} and Δ_{up2} in second cycle loading stage, respectively. Subsequently, the ELS will reduce to k_{r1} to start a new cycle, and it is quite different with the first one but similar to the other cycles later. In this model, a conservative analysis for self-centring ability is adopted, assuming the ε_{EDu2} equal to ε_{EDu1} . Therefore, a relatively underestimated value of P_{up2} , which is also the theoretical minimum value of P_{up2} , is defined as

$$P_{up2} = \frac{\tilde{b}}{h} (T_{in} + W - 2A_{ED}f(\varepsilon_{EDu1})) \quad (21)$$

$$\Delta_{up2} = P_{up2} / k_c \quad (22)$$

In a word, the analysis of self-centering bridge piers above develops a flag-shaped hysteretic response because of the combination of restoring ability provided by unbonded post-tensioned tendon and energy dissipation capacity provided by ED bars. The modified theoretical model can clearly identify various steps of lateral force-displacement analysis, and depict the whole process of stiffness degrading by introducing three damage factors.

3. Parametric Investigation

3.1. Pier parameter design

A parametric investigation was conducted based on the proposed theoretical model aforementioned, which emphasizes on three parameters including aspect ratio h/b , the initial pretension, T_{in} , and the ratio of ED bar, ρ_{ED} . In this study, the bridge piers have three aspect ratios $h/b = 2, 4, 6$. And the variation in the diameter and the ratio of ED bar are shown in Table.II. Besides, four unbonded post-tensioned tendons (1860 MPa in Chinese Code) have a diameter of 15.2 mm and an unbonded length of 2100 mm, and initial pretension around 12%, 24% and 36% of its yield strength were adopted to observe the influence of initial prestressing. To provide desirable energy dissipation capacity, an initial unbonded length l_{u0} of 100 mm was assumed in ED bars, and the equivalent unbonded length

l_{ED}^* can be calculated. The material properties are listed in Table.III, which are in conform with those of experiment.

The nomenclature of the investigated piers is described by the following example: [A4-T24- ED0.64] represents a pier with aspect ratio 4, pretension of 24% its yield strength, and ρ_{ED} of 0.64%.

3.2. Verification of the modified quasi-static response model

The modified quasi-static response model has been validated against the result of an existing experiment reported by Guo, Xin, He and Hu (2012)^[25]. The experimental study was based on an actual bridge project, whose bridge piers have a column with 5100 mm height, sectional area of 1200mm × 1200mm and a constant vertical load of 1960kN for each. In these experiments, we reduced scale with a coefficient of 1/3, so that we adopted a pier with 1700mm height, 400mm × 400mm sectional area, and 220 kN constant vertical load imposed on. As shown in Fig. 4, the profile of base was defined as 1400mm × 900mm × 500mm. The maximum horizontal displacement amplitude was limited at around 3.5% of column's height (about 60mm), and a cyclic multi-stage loading process was strictly executed during the experiment.

Table II Parameters in parametric investigation

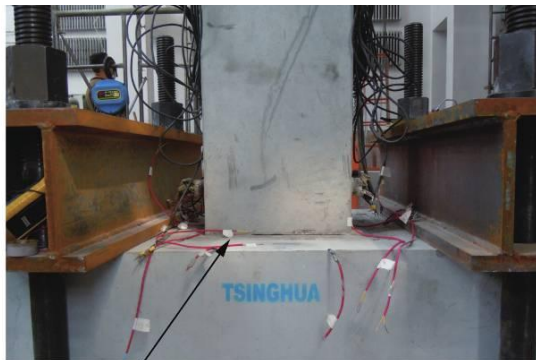
h/b	T_{in} (KN) (ratio of yield strength)	ρ_{ED} (%) (bar diameter)
2	160 (12%)	0.28 (12)
4	320 (24%)	0.50 (16)
6	480 (36%)	0.64 (18)
		0.79 (20)
		1.23 (25)

*Note: ρ_{ED} is the ratio of total sectional area of ED bars to the sectional area of concrete pier.

Table III Material properties in parametric investigation

f_{SCy} (MPa)	E_{SC} (MPa)	f_{EDy} (MPa)	f_{EDu} (MPa)	E_{EDu} (MPa)	α_{ED}
1860	21000	335	550	20600	0.01

*Note: α_{ED} is the post-yield stiffness Ratio



Joint: discontinuous contact between the LB component and base.



SC components: anchoring on the top.

Fig. 4 Experimental specimen (Conducted by Tsinghua University)

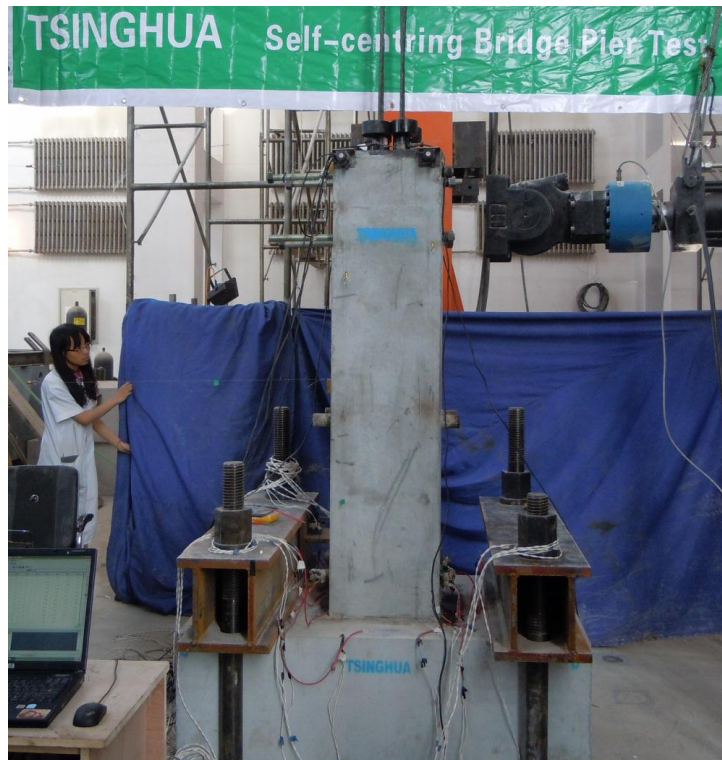


Fig. 5 Experimental specimen (Conducted by Tsinghua University)

As a combination of the desirable self-centering capacity with the appreciable energy dissipation capacity, the curve displayed a typical flag-shape hysteretic response resulting in negligible residual displacement. The lateral stiffness of the system and self-centering capacity gradually degrades with the increase in cycle, which can be explained by the damage of concrete edge and accumulation of equivalent plastic strain in ED components. Consistent with the stiffness degrading analysis of the proposed modified theoretical model, the center of rotation moved inside leading to the reduction of restoring moment, and the concrete cover were pulled off resulting in the reduction of lateral stiffness. Furthermore, the increase of equivalent unbonded length of ED components gives rise to the stiffness degrading at the same time. The comparison of the result between modified quasi-static response model and the experiment is shown in Fig. 6, where good agreement is clearly evident including the stiffness degrading process.

3.3. Cyclic loading analysis

Cyclic loading analysis was performed on a series of piers based on lateral force-displacement analysis described previously.

The result of all cyclic loading curves were rearranged and presented in Fig. 7. As shown in Fig. 7(a), the ultimate strength of piers proportionally increase with ρ_{ED} , and it is evident that adding ED bars can be beneficial to resist a rare earthquake. Besides, increasing initial pretension is also effective to this end. Fig. 7(b) shows that increasing T_{in} can conspicuously delay the uplifting of SCP, which is significant to the piers required for lifeline bridges.

Because there will be a noticeable reduction of ELS after the uplifting of piers, and the lateral displacement may subsequently increase quickly to exceed the design limit. Moreover, the opening of critical interface will further expose the vulnerable part of the piers to corrosive substances in some specific environment like coastal region.

Another important indicator for serviceability is the strength and drift corresponding to yielding point. Yielding point is associated with a drastic softening of the pier. In the modified quasi-static response model established previously, it is defined as P_{y1} and Δ_{y1} when the outer ED bars come to yield. Fig. 7 (c) and (d) show that higher initial pretension and ρ_{ED} can effectively delay the yielding of SCP. As the analysis aforementioned, all components of the piers will behave elastically if the lateral displacement can be limited within Δ_{y1} . As a result,

Δ_{y1} can be a desirable drift limit for serviceability design.

Moreover, an investigation of self-centering and energy dissipation capacity was performed. Only the result of three groups with an aspect ratio of 4 was shown in Fig. 8, because the change of aspect ratio does not prevail in this investigation. If there is an ideal combination of ED bars and SC tendons, a desirable seismic performance of SCP can be achieved. That is, the pier can exhibit a flagshape hysteretic response with little to no residual displacement and have a relatively higher energy dissipation capability at the same time. As shown in Fig. 8, the bold line represents the optimum ρ_{ED} values suited for three different scenarios with increasing pretension value.

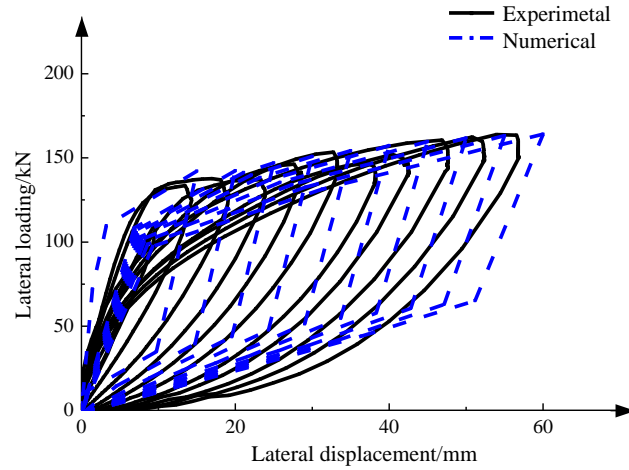


Fig. 6 Comparison between experimental results and modified quasi-static response model results

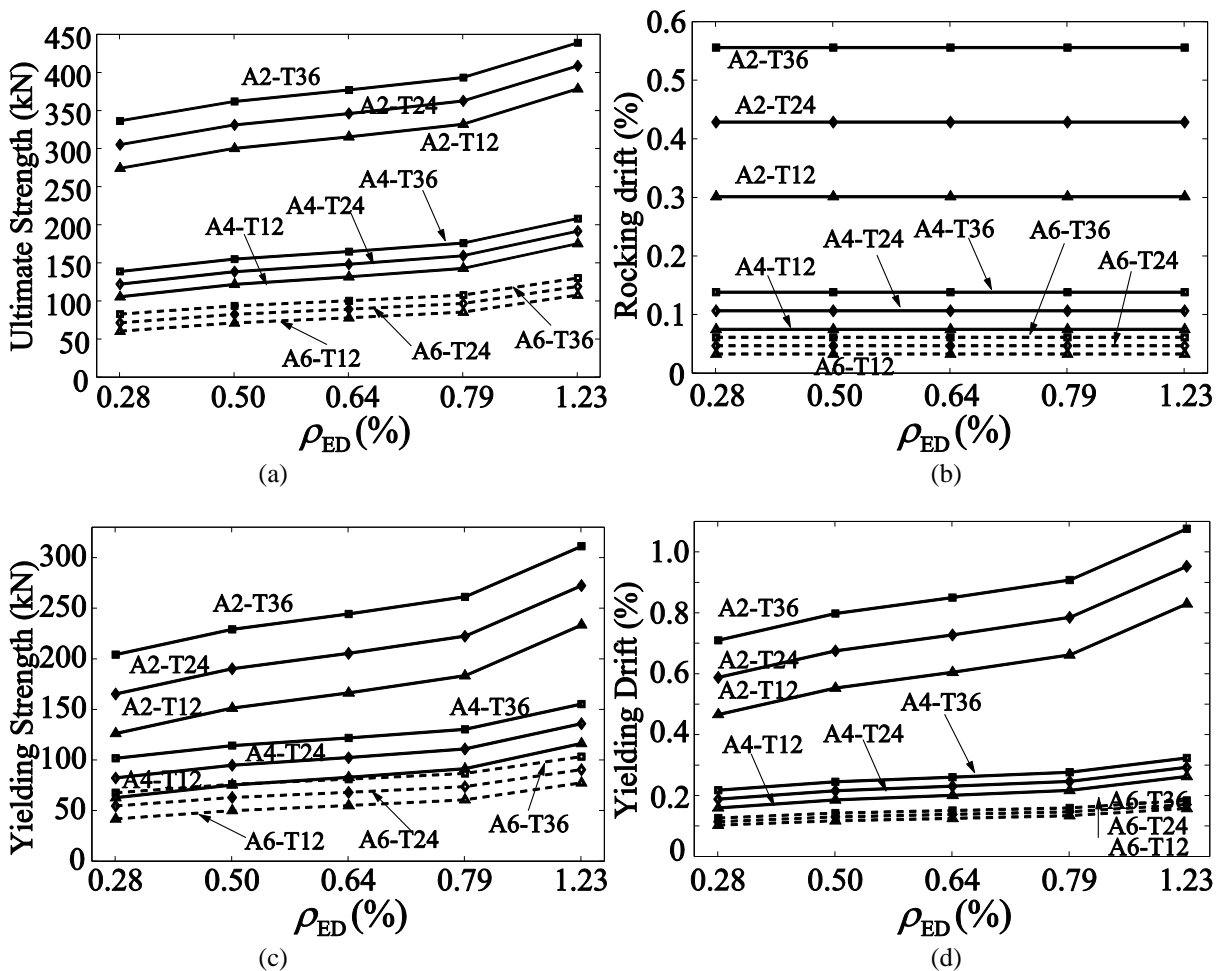


Fig. 7 Results of cyclic loading analysis

The self-centering effect can be evaluated with the value of residual displacement, which is the permanent plastic displacement when lateral force comes back to zero. In Fig. 8(a), the residual displacement increases rapidly with the increase of ρ_{ED} , and the similar trend can be identified in other groups. While only little residual displacement exists with a ρ_{ED} of 0.50%, a remarkable residual displacement over 30mm (1.9% drift), which is

unacceptable for any further safety of bridges, will be produced with a ρ_{ED} of 0.79%. On the contrary as shown in Fig. 8(c), 0.79% is just the optimum value of ρ_{ED} indicating no noticeable residual displacement remains after cyclic loading. Consistent with the prediction of lateral force-displacement analysis, increasing pretension will contribute to the self-centering capacity and

subsequently a higher optimum ρ_{ED} values can be found in this study. Besides, it is evident that as ρ_{ED} increases, the energy dissipation capacity increases as shown by the area surrounded by hysteretic curves. As a result, an appropriate ρ_{ED} should be first determined according to energy dissipation demand in the seismic design, because the change of ρ_{ED} will have contradictory effects on self-centering and energy dissipation capacity at the same time. And then, a required pretension can be determined on the basis of ED design to limit residual displacement within an acceptable extent.

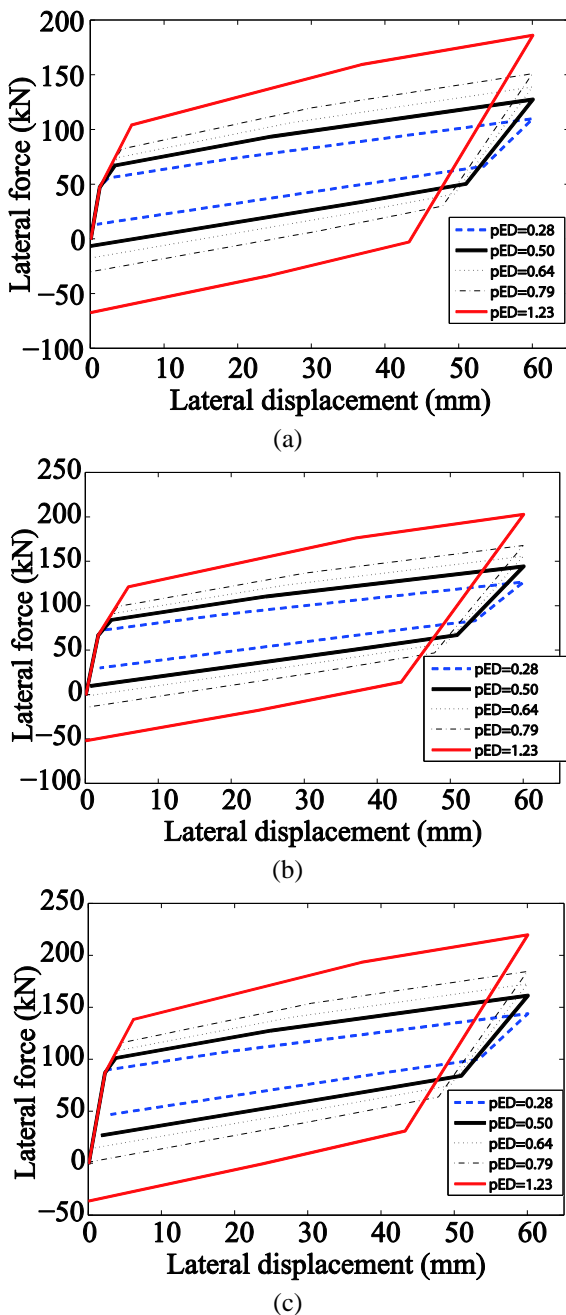


Fig. 8 Investigation of self-centering and energy dissipation capacity.

4. Conclusions

This paper established a modified quasi-static response model for self-centering concrete bridge piers, which can depict the stiffness degrading process by introducing three damage factors. The proposed modified quasi-static response model with damage mechanism has been validated against experiment we conducted previously, and a series of parameter investigation has been raised based on this model. Important conclusions are summarized as follows.

(1) The modified quasi-static response model of the self-centering concrete pier incorporating gradual lateral stiffness deterioration has been investigated and compared through quasi-static analysis. The experimental result shows that the self-centering concrete pier sustains substantial lateral loading. The residual displacement after loading has been reduced effectively in the reported self-centering pier case. The proposed modified quasi-static response model with damage mechanism has been validated against experiment, where a good agreement is clearly evident.

(2) The observed lateral stiffness deterioration was modeled in the comprehensive modified model for lateral force-displacement curve. Three damage factors are effective in incorporating the stiffness deterioration with respect to the structural damage. β_u , β_c and β_r can feasibly describe the elongation of equivalent unbonded length of ED bars, the reduction of initial lateral stiffness of piers and the decrease of equivalent arm of force, respectively.

(3) The theoretical lateral force-displacement analysis was completely depicted in this paper. The Equations of lateral load and displacement for various steps in cyclic analysis have been clearly illustrated, which develops a typical flag-shaped hysteretic response and the whole process of stiffness deterioration. The difference of uplifting load between first and second round cycles were identified, because the mild steel in compression inevitably offsets part of bridge weight and pretension after first cycle.

(4) A parameter investigation based on cyclic loading analysis was conducted, focusing on three parameters including aspect ratio, the initial pretension, and the ratio of ED bar. Limiting the aspect ratio is critical to improve the seismic performance, while increasing initial pretension and ratio of ED bar can contribute to increasing pier's ultimate strength and yielding strength. As to residual displacement, initial pretension is beneficial and has no relevance with energy dissipation capacity, however, the ratio of ED bar has counter impact on self-centering and energy dissipation capacities at the same time. Therefore, it is suggested that an appropriate ratio of ED bar first be designed according to energy dissipation demand, then a lower bound of initial pretension to eliminate residual displacement can be easily achieved through Eq.(20).

Acknowledgement: The authors want to thank the consistent support from projects of NSFC (National Science Foundation of China) under grant number

51378292 and 51038006 and a project of Beijing Natural Science Foundation under grant number 8144051. Thanks to the support from the National Science Foundation of China under contrast number U1134110 which was co-lead by late Professor Kegui Xin (1950-2012) and Dr. Minghua He for the seismic research on High Speed Rail concrete bridge pier. Professor Gexue Ren is highly appreciated. The project is also supported by China Postdoctoral Science Foundation First Class Project 2013M530048. Any opinions expressed in this paper are those of the authors and not necessarily of the sponsors.

References

- [1] Wang ZF. A preliminary report on the Great Wenchuan Earthquake, *Earthquake Engineering and Engineering Vibration*, 2008, No. 2, Vol. 7, pp. 225-234.
- [2] W. Phillip Yen, Chen G, Yashinski M, Hashash Y, Holub C, Kehai W, Guo XD. Lessons in bridge damage learned from the Wenchuan earthquake, *Earthquake Engineering and Engineering Vibration*, 2009, No. 2, Vol. 8, pp. 275-285.
- [3] Kawashima K, MacRae G, Hoshikuma J, Nagaya K. Residual displacement response spectrum, *Journal of Structural Engineering* 1998, No. 5, Vol. 124, pp. 523-530.
- [4] Luco N, Bazzurro P, et al. Dynamic versus static computation of the residual capacity of mainshockdamaged building to withstand an aftershock, *Proceedings of the 13th World Conference on Earthquake Engineering*, Vancouver, Canada, 2004.
- [5] Lee WK, Billington SL. Performance-based earthquake engineering assessment of a self-centering, post-tensioned concrete bridge system, *Earthquake Engineering and Structural Dynamics*, 2011, No. 8, Vol. 40, pp. 887-902.
- [6] Guo J. Performance Based Research on the Seismic Theory and Test of New Self-Centering Pier. [Master Thesis] Beijing, China, Tsinghua University, 2012.
- [7] He MH, Xin KG, Guo J, Guo YJ. Research on the intrinsic lateral stiffness and hysteretic behavior of selfcentering pier, *China Railway Science*, 2012, No. 5, Vol. 36, pp. 22-27.
- [8] Kawashima K. The 1996 Japanese seismic design specifications of highway bridges and the performance based design, *Seismic Design Methodologies for the Next Generation of Codes*, Bled, Slovenia, 1997, pp. 371-382.
- [9] Bazzurro P, Cornell C, et al. Guidelines for seismic assessment of damaged buildings, *Proceedings of the 13th World Conference on Earthquake Engineering* couer, Canada, 2004.
- [10] Billington SL, Yoon JK. Cyclic response of unbonded posttensioned precast columns with ductile fiber-reinforced concrete, *Journal of Bridge Engineering*, ASCE, 2004, No. 4, Vol. 9, pp. 353-363.
- [11] GB50111-2006. Code for seismic design of railway engineering, China Ministry of Railways, 2009.
- [12] Christopoulos C, Pampanin S. Towards performance-based design of MDOF structures with explicit consideration of residual deformations, *ISET Journal of Earthquake Technology*, 2004, No. 1, Vol. 41, pp. 53-73.
- [13] Fib. Seismic design of precast concrete building structures. Lausanne, Switzerland, International Federation for Structural Concrete, 2003.
- [14] Kim HJ, Christopoulos C. Friction damped posttensioned self-centering steel moment-resisting frames, *Journal of Structural Engineering*, ASCE, 2008, No. 11, Vol. 134, pp. 1768-1779.
- [15] MacRae GA, Kawashima K. Post-earthquake residual displacement of bilinear oscillators, *Earthquake Engineering and Structural Dynamics*, 1997, No. 7, Vol. 26, pp. 701-716.
- [16] Marriott D, Pampanin S, Palermo A. Quasi-static and pseudo-dynamic testing of unbonded post-tensioned rocking bridge piers with external replaceable dissipaters, *Earthquake Engineering and Structural Dynamics*, 2009, No. 3, Vol. 38, pp. 331-354.
- [17] Palermo A, Pampanin S. Enhanced seismic performance of hybrid bridge systems: comparison with traditional monolithic solutions, *Journal of Earthquake Engineering*, 2008, No. 8, Vol. 12, pp. 1267-1295.
- [18] Palermo A, Pampanin S, Calvi GM. Concept and development of hybrid solutions for seismic resistant bridge systems, *Journal of Earthquake Engineering*, 2005, No. 6, Vol. 9, pp. 899-921.
- [19] Palermo A, Pampanin S, Marriott D. Quasi-static tests of seismic resistant bridge piers with hybrid connections: comparison with monolithic solutions, *Proceedings of the 2nd International FIB Congress*, Naples, Italy, June, 2006.
- [20] Palermo A, Pampanin S, Carr A. Efficiency of simplified alternative modelling approaches to predict the seismic response of precast concrete hybrid systems, *Proceedings of fib symposium "Keep Concrete Attractive"*, Budapest.
- [21] Pampanin S, Christopoulos C, Priestley MJN. Residual deformations in the performance-based seismic assessment of frame structures, *Research Report Rose 2002/02 European School for Advanced Studies on Reduction of Seismic Risk*, Pavia, Italy, 2002.
- [22] Pollino M, Bruneau M. Seismic retrofit of bridge steel truss piers using a controlled rocking approach, *Journal of Bridge Engineering*, ASCE, 2007, No. 5, Vol. 12, pp. 600-610.
- [23] Ou YC, Chiewanichakorn M, Aref AJ, Lee GC. Seismic performance of segmental precast unbonded posttensioned concrete bridge columns, *Journal of Structural Engineering*, ASCE, 2007, No. 11, Vol. 133, pp. 1636-1647.
- [24] He MH, Xin KG, Guo J. Local stability study of new bridge piers with self-centering joints, *Engineering Mechanics*, 2012, No. 4, Vol. 29, pp. 122-127.
- [25] Guo J, Xin KG, He MH, Hu L. Experimental study and analysis on the seismic performance of a self-centering bridge pier, *Engineering Mechanics*, 2012, No. s2, Vol. 29, pp. 29-34, 45.
- [26] Raynor DJ, Lehman DE, Stanton JF. Bond-slip response of reinforcing bars grouted in ducts, *ACI Structure Journal*, 2002, No. 5, Vol. 99, pp. 568-576.
- [27] Yu-Chen Ou, Mu-Sen Tsai, Kuo-Chun Chang, George C. Lee. Cyclic behavior of precast segmental concrete bridge columns with high performance or conventional steel reinforcing bars as energy dissipation bars, *Earthquake Engineering & Structural Dynamics*, 2010, Vol. 39, pp. 1181-1198.